Displaying a high-resolution digital hologram on a low-resolution spatial light modulator with the same resolution obtained from the hologram

P.W.M. Tsang,[1*] T.-C. Poon,[2,3] and C. Zhou[3]

[1]*Department of Electronic Engineering, City University of Hong Kong, Hong Kong China*
[2]*Bradley Department of Electrical and Computer Engineering, Virginia Tech, Blacksburg, VA 24061, USA*
[3]*Shanghai Institute of Optics and Fine Mechanics, Chinese Academy of Sciences, P.O. Box 800-211, Shanghai 201800, China*
[*]*eewmtsan@cityu.edu.hk*

Abstract: In this paper, a fast method for displaying a digital, real and off-axis Fresnel hologram on a lower resolution device is reported. Preserving the original resolution of the hologram upon display is one of the important attributes of the proposed method. Our method can be divided into 3 stages. First, a digital hologram representing a given three dimensional (3D) object is down-sampled based on a fix, jitter down-sampling lattice. Second, the down-sampled hologram is interpolated, through pixel duplication, into a low resolution hologram that can be displayed with a low-resolution spatial light modulator (SLM). Third, the SLM is overlaid with a grating which is generated based on the same jitter down-sampling lattice that samples the hologram. The integration of the grating and the low-resolution hologram results in, to a good approximation, the resolution of the original hologram. As such, our proposed method enables digital holograms to be displayed with lower resolution SLMs, paving the way for the development of low-cost holographic video display.

OCIS codes: (090.0090) Holography; (090.1995) Digital holography; (090.1760) Computer holography.

References and links

1. J. Weng, T. Shimobaba, N. Okada, H. Nakayama, M. Oikawa, N. Masuda, and T. Ito, "Generation of real-time large computer generated hologram using wavefront recording method," Opt. Express **20**(4), 4018–4023 (2012).
2. P. Tsang, W. K. Cheung, T.-C. Poon, and C. Zhou, "Holographic video at 40 frames per second for 4-million object points," Opt. Express **19**(16), 15205–15211 (2011).
3. M. Stanley et al., "100-megapixel computer-generated holographic images from Active Tiling: a dynamic and scalable electro-optic modulator system," SPIE5005, 247–258 (2003).
4. N. Collings, "Optically Addressed Spatial Light Modulators for 3d Display," J. Nonlinear Opt. Phys. Mater. **20**(4), 453–457 (2011).
5. C. Slinger, C. Cameron, and M. Stanley, "Computer-Generated Holography as a Generic Display Technology," Computer **38**(8), 46–53 (2005).
6. H-S. Lee, H. Song, S. Lee, N. Collings, and D. Chu, "High resolution spatial light modulator for wide viewing angle holographic 3D display", Coll. Conf. 3D Res., (CC3DR), 71–72, (2012).
7. P. W. Tsang, T.-C. Poon, C. Zhou, and K. W. Cheung, "Binary Mask Programmable Hologram," Opt. Express **20**(24), 26480–26485 (2012).
8. D. E. Golberg, *Genetic Algorithms in Search, Optimization, and Machine Learning*, Addison Wesley, (1989).
9. R. L. Cook, "Stochastic sampling in computer graphics," ACM Trans. Graph. **5**(1), 51–72 (1986).
10. A. V. Balakrishnan, "On the problem of time jitter in sampling," IRE Trans. Inf. Theory **8**(3), 226–236 (1962).
11. M. A. Z. Dippé and E. H. Wold, "Antialiasing Through Stochastic Sampling," SIGGRAPH **19**(3), 69–78 (1985).

1. Introduction

With the advancement of computing technology, digital holography has undergone rapid and encouraging development in the past two decades. To date, a medium size digital Fresnel

#190252 - $15.00 USD Received 8 May 2013; revised 18 Jun 2013; accepted 6 Jul 2013; published 16 Jul 2013

hologram can be generated numerically swiftly based on a commodity personal computer (PC) [1,2]. However, there is a lack of devices for displaying the hologram which generally requires a resolution of over 2400dpi (about 10 microns) to provide an observable reconstructed image. Existing spatial light modulators (SLMs), such as the Liquid Crystal on Silicon (LCoS), are small in size and rather expensive. Although both the resolution and size of these devices can be enhanced with the use of multiple units, or the active tiling (AT) method [3–6], the complexity and cost of the setup is increased substantially. A solution to address the above problems has been proposed by Tsang et al. [7] with the concept of binary mask programmable hologram (BMPH). The BMPH is formed by overlaying a fixed, high-resolution binary grating onto a low-resolution binary mask. By generating the correct binary mask through an iterative process based on Simple Genetic Algorithm (SGA) [8], the BMPH can mimic a hologram with identical resolution as the grating, thereby capable of reconstructing an image with the same resolution of the original hologram. As the binary mask can be displayed with a less stringent display device of lower resolution, the cost and complexity of implementing the holographic display (either as a single or a tiling structure) can be reduced. However, the BMPH method suffers from 3 major problems that severely limit its application in practice. First, the computer memory, as well as the time taken to compute the binary mask is overwhelming. Second, so far only small on-axis hologram of size 256x256 pixels can be realized. For larger holograms, the correct mask cannot be found even after prolong period of computations, probably due to the difficulty in locating the optimal solution in the search space with the SGA. Third, for certain object images, the method fails to generate the correct binary mask even after large number of iterations. Despite all these shortcomings, the BMPH has casted light on the feasibility of using a low-resolution SLM to reconstruct an image obtained from the higher resolution of the original hologram. In this paper, we follow the concept of the BMPH and propose a fast method for displaying an off-axis digital hologram with a lower resolution SLM. Our proposed method, together with the experimental evaluation, are presented in sections 2 and 3, respectively. Finally, a conclusion is given in section 4, summarizing the essential findings.

2. Proposed method

Our proposed method can be divided into 3 stages as shown in Fig. 1. The input is an amplitude, off-axis digital Fresnel hologram $H(x,y)$ that is generated as follows. Given a 3-D object scene comprising of P object points, a complex hologram $H_C(x,y)$ is first derived with the Fresnel diffraction equation shown in Eq. (1).

$$H_C(x,y)=\sum_{j=0}^{P-1} a_j \exp\left(\frac{i2\pi}{\lambda}\sqrt{(x-x_j)^2\delta^2+(y-y_j)^2\delta^2+z_j^2}\right), \tag{1}$$

where λ is the wavelength of the optical beam, and (x,y) being the horizontal and vertical coordinates of the hologram plane. The terms a_j, (x_j,y_j), and z_j denote the intensity, the horizontal and vertical co-ordinates on the vertical plane, and its axial distance from the hologram, of the *jth* object point, respectively. The hologram pixel is assumed a square shape with side length δ. Subsequently, the complex hologram is converted into a real, off-axis hologram $H(x,y)$ by multiplying with an off-axis plane reference wave $R(y)=\exp(i2\pi y\delta\sin\theta/\lambda)$, and taking the real part of the product as

$$H(x,y)=\text{Real}\left[H_C(x,y)R(y)\right]. \tag{2}$$

In the optical experiments that follow, the off-set angle θ is taken to be 1.2^{o}

#190252 - $15.00 USD Received 8 May 2013; revised 18 Jun 2013; accepted 6 Jul 2013; published 16 Jul 2013

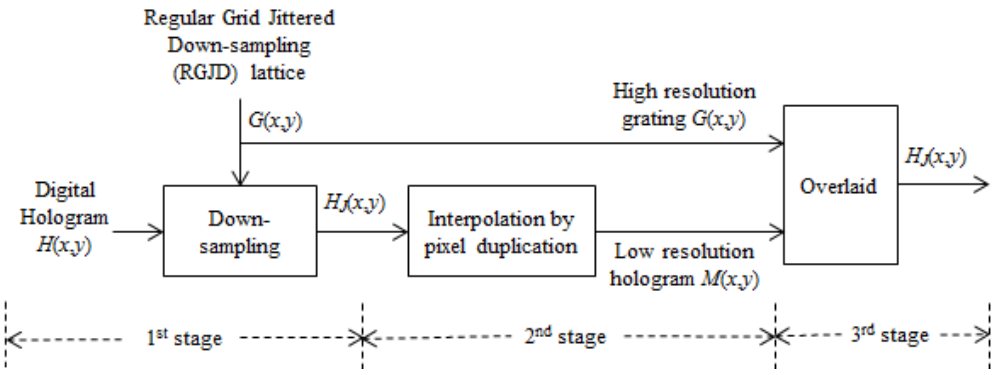

Fig. 1. Proposed method for generating the low-resolution hologram and the high resolution grating.

In the first stage, we apply the "regular grid jittered down-sampling" (RGJD) [9–11] to the input digital hologram. In RGJD, the sampling instance of a regular lattice is shifted to a random position within the sampling interval (a process commonly referred to as jittering). According to the analysis in [9–11], the RGJD results in significant reduction in aliasing errors if the jitters are uncorrelated to the signal, thereby preserving the basic composition of the signal spectrum. On the downside, high frequency contents are attenuated, and uniform noise is imposed on the sampled signal. As the analysis on RGJD has been reported in many literatures, such as [11], the details will not be reiterated here. Instead, we shall focus on the effect of RGJD on the signal spectrum. Given an arbitrary one dimensional (1-D) signal $s(x)$, applying the RGJD results in a down-sampled signal $s_d(x)$ given by Eq. (3).

$$s_d(x) = \begin{cases} s(x)\,(\text{sample point}) & x = km + \tau_1 \\ 0 & otherwise \end{cases}, \tag{3}$$

where k is the sampling interval, m is a positive integer, and $0 \le \tau_1 < k$ is a random integer. Let $S(\omega)$, $S_d(\omega)$, and $\varphi(\omega)$ denote the frequency spectrums of $s(x)$, $s_d(x)$, and the sampling lattice, respectively. According to [11], if the random variable τ_1 is uncorrelated to $s(x)$, $S_d(\omega)$ can be expressed in Eq. (4) as

$$\begin{aligned} S_d(\omega) &= S(\omega) * \phi(\omega) = S(\omega) * \left[\frac{1}{k}\left(1 - \sin c^2(\omega/2k)\right)\right] + \frac{2\pi}{k^2} S(\omega) \\ &= S(\omega) * \frac{N_j(\omega)}{k} + \frac{2\pi}{k^2} S(\omega), \end{aligned} \tag{4}$$

where $sinc(x) = \sin x / x$. The term $N_j(\omega) = \left[\left(1 - \sin c^2(\omega/2k)\right)\right]$ is a term which is zero at $\omega = 0$, and increases with frequency. The convolution of $S(\omega)$ and $N_j(\omega)$ results in the jittered noise. From Eq. (4), it can be inferred that the signal and the noise strength are decreased by factors of k^2 and k, respectively. In addition, $S_d(\omega)$ is free from the aliasing error. The 1-D RGJD can be easily extended to down-sample a 2-D hologram. The hologram is uniformly partitioned into non-overlapping square blocks of size $k \times k$ pixels, where k is the sampling interval. Within each block, a single pixel is sampled at random, while the rest

#190252 - $15.00 USD Received 8 May 2013; revised 18 Jun 2013; accepted 6 Jul 2013; published 16 Jul 2013

are set to 0 (i.e., opaque). Mathematically, this process can be represented by multiplying $H(x,y)$ with a RGJD lattice $G(x,y)$ given by Eq. (5).

$$G(x,y)=\begin{cases}1\,(\textit{sample point}) & x=mk+\tau_1 \text{ and } y=nk+\tau_2\\ 0 & \textit{otherwise}\end{cases}, \tag{5}$$

where m,n are integers. τ_1,τ_2 are random integers that are smaller than k. The down-sampled hologram $H_J(x,y)$ is the product of $H(x,y)$ with $G(x,y)$ as shown in Eq. (6)

$$H_J(x,y)=H(x,y)G(x,y). \tag{6}$$

As we shall demonstrate later, the reconstructed image of a jittered down-sampled hologram is similar to the one obtained with the original hologram. In the second stage, an interpolated image $M(x,y)$ is derived from $H_J(x,y)$ by filling the blanked pixels in each block of $H_J(x,y)$ with the value of the sampled pixel (i.e., interpolation by pixel duplication). $M(x,y)$ is composed of non-overlapping $k\times k$ square blocks, each with a homogeneous intensity equal to the value of the sampled pixel in $H_J(x,y)$. Each block can be taken as a pixel in $M(x,y)$ with a dimension that is k times larger than that of the pixel in $H_J(x,y)$ along both the horizontal and the vertical directions. In another words, the effective resolution of $M(x,y)$ is only $1/k\,th$ of that of the original hologram, and can be displayed with a device of relatively lower resolution. In the third stage, we note that $H_J(x,y)$ can be obtained with the product of $M(x,y)$ and $G(x,y)$, as given in Eq. (7).

$$H_J(x,y)=M(x,y)G(x,y). \tag{7}$$

As such, the jittered sampled hologram can be realized by overlaying the grating $G(x,y)$ onto the low resolution hologram $M(x,y)$. For the sake of clarity, the above process is illustrated with Figs. 2(a) to 2(d). A small 4×4 hologram $H(x,y)$, and a grating $G(x,y)$ corresponding to a RGJD lattice with sampling interval $k=2$, are shown in Figs. 2(a) and 2(b), respectively. In the grating image $G(x,y)$, sampled pixels (with value '1') are shaded in white and non-sampled pixels (with value '0') are shaded in black. The down-sampled hologram $H_J(x,y)$, obtained by the product of $G(x,y)$ and $H(x,y)$ (Eq. (7)), is shown in Fig. 2(c). The interpolated hologram $M(x,y)$ is shown in Fig. 2(d). $M(x,y)$ is generated by duplicating the sampled values in $G(x,y)$ within each $k\times k$ square block. It can be easily seen that the jittered down-sampled hologram $H_J(x,y)$ can be obtained through the product of $H(x,y)$ and $G(x,y)$ [See Eq. (6)] or equivalently the product of $M(x,y)$ and $G(x,y)$ [See Eq. (7)]. The expected result of the proposed method is as follows: $M(x,y)$, being the low-resolution of the hologram (has been down-sampled and through interpolation) is displayed on a SLM. The RGJD grating $G(x,y)$, of the same resolution as the original hologram, is placed immediately against the SLM for display as shown in Fig. 3. Upon illumination with a planar optical wave, the reconstructed image will have the same resolution as that obtained from the original hologram. In the next section, we show results to substantiate our claim.

#190252 - $15.00 USD Received 8 May 2013; revised 18 Jun 2013; accepted 6 Jul 2013; published 16 Jul 2013

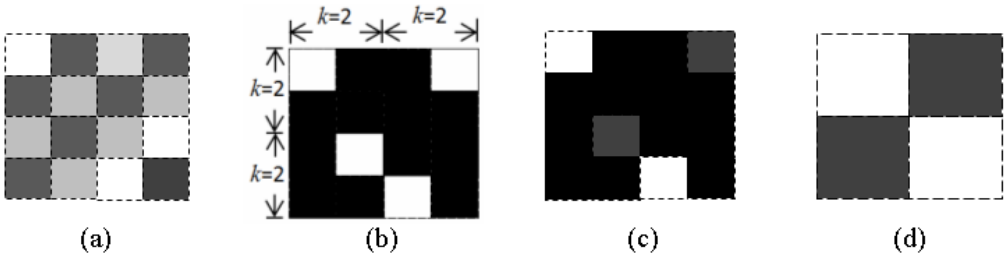

Fig. 2. (a) A digital hologram $H(x,y)$. (b) The RGJD lattice $G(x,y)$, which is also adopted as the grating. In each 2×2 square block, there is only one sampled pixel (the white pixel). (c) The hologram $H_J(x,y)$ obtained by down-sampling $H(x,y)$ with $G(x,y)$. (d) The low resolution hologram $M(x,y)$ obtained by filling each $k\times k$ square block in $H_J(x,y)$ with the sampled pixel.

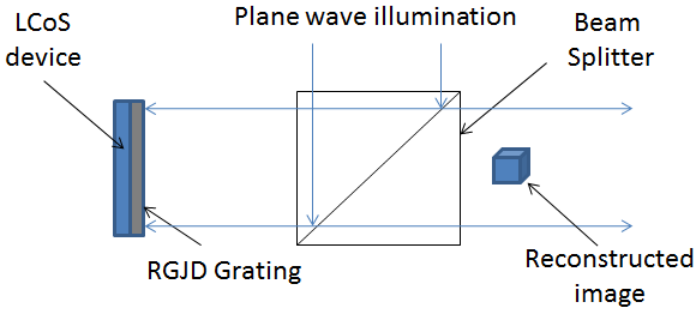

Fig. 3. Optical setup of the LCoS device, the grating, and the illumination

3. Experimental results

Our proposed method is evaluated with an off-axis digital hologram $H(x,y)$ comprising of 2048×2048 pixels, representing the planar image "Lenna eyes" shown in Fig. 4(a). The image is parallel to, and at an axial distance of 0.6m from the hologram. The latter has a pixel size of $7u\text{m}\times7u\text{m}$, and is generated with $\lambda=650u\text{m}$. The reference plane wave $R(y)$ is inclined at an angle of 1.2^{o} along the vertical direction. The numerical reconstructed image at the focal plane is shown in Fig. 4(b). Next, we simulate the outcome when the hologram is displayed with a device of coarser resolution, having a pixel size of $14\mu\text{m}\times14\mu\text{m}$. This is accomplished by down-sampling the hologram with a factor of 2 along both the horizontal and vertical directions, so that effective pixel separation is $14\mu\text{m}\times14\mu\text{m}$. The numerical reconstructed image of the decimated hologram is shown in Fig. 4(c). Due to the reduction of the hologram resolution, the quality of the reconstructed image is very poor, and the Peak Signal to Noise Ratio (PSNR) as compare with the reconstructed image in Fig. 4(b) is only 11.2dB. To evaluate our proposed method, we apply RGJD (i.e., Eq. (3)) to down-sample the hologram $H(x,y)$ with a factor of 2. The RGJD lattice $G(x,y)$ is taken as the high resolution binary grating. Subsequently, the down-sampled hologram, denoted by $H_J(x,y)$, is interpolated to a lower resolution hologram $M(x,y)$ with pixel duplication. With a factor of $k=2$, the effective pixel size of $M(x,y)$ is $14\mu\text{m}\times14\mu\text{m}$. As explained previously, $H_J(x,y)$ can be realized by overlaying the binary grating $G(x,y)$ onto the low resolution

#190252 - $15.00 USD Received 8 May 2013; revised 18 Jun 2013; accepted 6 Jul 2013; published 16 Jul 2013

hologram $M(x,y)$. Hence, evaluating $H_J(x,y)$ will be equivalent to the evaluation of the integration of $G(x,y)$ and $M(x,y)$. The numerical reconstructed image of $H_J(x,y)$ is shown in Fig. 4(d). We observe that apart from some noise contamination and blurring, the reconstructed image is similar to that derived from the original hologram, and having a PSNR of 23.85dB. Referring to Eq. (4), it can be inferred that further increasing the sampling factor is not preferred as the signal strength will be decreased substantially. However, for the sake of interest, we evaluate the result for $k=3$, increasing the effective pixel size to $21\mu\text{m}\times 21\mu\text{m}$. The numerical reconstructed image is shown in Fig. 4(e). Although the quality of the image is still acceptable, the noise contamination becomes more prominent, and the PSNR drops by almost 3dB to 20.89dB.

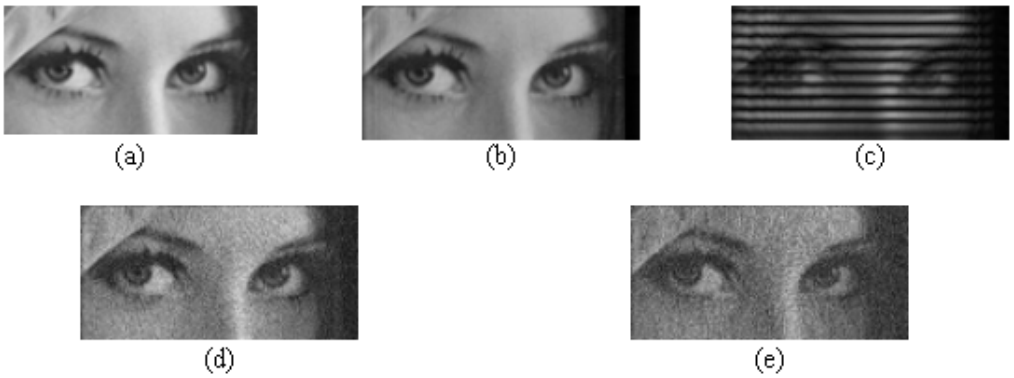

Fig. 4. (a) Source image "Lenna eyes". (b) Numerical reconstruction of original hologram representing the image in Fig. 4(a). (c) Numerical reconstruction of the original hologram after down-sampling by 2 times with a uniform sampling lattice. (d) Numerical reconstruction of the original hologram after down-sampling by 2 times with the RGJD lattice. (e) Numerical reconstruction of the original hologram after down-sampling by 3 times with the RGJD lattice.

4. Conclusion

In our proposed method, we apply RGJD and interpolation to convert a real, off-axis digital Fresnel hologram into a low-resolution hologram. By overlaying the low-resolution hologram with a binary grating that is generated based on the same RGJD lattice, a good approximation of the original hologram can be realized. The process only involves negligible amount of computation and is not restricted by the size and content of the hologram. Deriving the RGJD lattice and its associated binary grating is an off-line process, and once generated, they can be applied universally to all the input holograms. Experimental evaluation reveals that with our proposed method, the reconstructed image of a hologram can be preserved favorably after its resolution has been decreased to one third of its original value. The encouraging result suggests that such technique can be readily applied to enable high-resolution holograms to be display on a relatively lower resolution device.

Acknowledgment

This work is supported by the Chinese Academy of Sciences Visiting Professorships for Senior International Scientists Program under Grant Number 2010T2G17 and the High-End Foreign Experts Recruitment Program, China, under Grant Number GDJ 20130491009.

#190252 - $15.00 USD Received 8 May 2013; revised 18 Jun 2013; accepted 6 Jul 2013; published 16 Jul 2013